

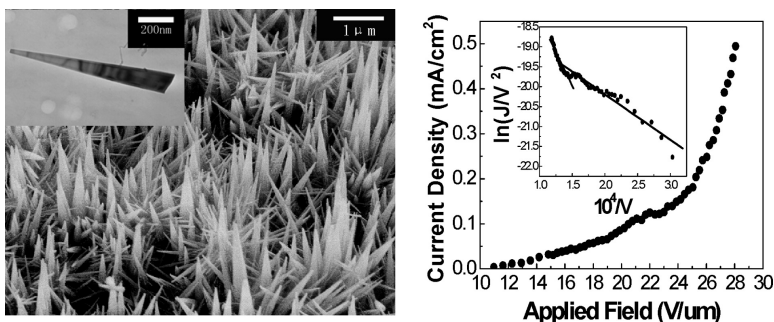
Article

## Vapor–Solid Growth and Characterization of Aluminum Nitride Nanocones

Chun Liu, Zheng Hu, Qiang Wu, Xizhang Wang, Yi Chen,  
 Hai Sang, Jianmin Zhu, Shaozhi Deng, and Ningsheng Xu

*J. Am. Chem. Soc.*, **2005**, 127 (4), 1318-1322 • DOI: 10.1021/ja045682v • Publication Date (Web): 07 January 2005

Downloaded from <http://pubs.acs.org> on March 24, 2009



### More About This Article

Additional resources and features associated with this article are available within the HTML version:

- Supporting Information
- Links to the 25 articles that cite this article, as of the time of this article download
- Access to high resolution figures
- Links to articles and content related to this article
- Copyright permission to reproduce figures and/or text from this article

[View the Full Text HTML](#)

## Vapor–Solid Growth and Characterization of Aluminum Nitride Nanocones

Chun Liu,<sup>†</sup> Zheng Hu,<sup>\*†</sup> Qiang Wu,<sup>†</sup> Xizhang Wang,<sup>†</sup> Yi Chen,<sup>†</sup> Hai Sang,<sup>‡</sup> Jianmin Zhu,<sup>‡</sup> Shaozhi Deng,<sup>§</sup> and Ningsheng Xu<sup>§</sup>

Contribution from the Key Laboratory of Mesoscopic Chemistry of MOE and Jiangsu Provincial Lab for NanoTechnology, Department of Chemistry, and National Laboratory of Solid State of Microstructures, Department of Physics, Nanjing University, Nanjing 210093, and State Key Laboratory for Optical and Electric Materials and Technology, Zhongshan University, Guangzhou 510275, China

Received July 19, 2004; E-mail: zhenghu@nju.edu.cn

**Abstract:** Aluminum nitride nanostructures are attractive for many promising applications in semiconductor nanotechnology. Herein we report on vapor–solid growth of quasi-aligned aluminum nitride nanocones on catalyst-coated wafers via the reactions between  $\text{AlCl}_3$  vapor and  $\text{NH}_3$  gas under moderate temperatures around 700 °C, and the growth mechanism is briefly discussed. The as-prepared wurtzite aluminum nitride nanocones grow preferentially along the *c*-axis with adjustable dimensions of the sharp tips in the range of 20–60 nm. The photoluminescence spectrum reveals a broad blue emission band with a fine photon structure while the field emission study shows a notable emission current with a moderate turn-on field as expected, suggesting their potential applications in light and electron emission nanodevices.

### Introduction

Since the discovery of carbon nanotubes (CNTs),<sup>1</sup> the nanotubular family has been rapidly extended to different layered compounds including nitrides,<sup>2</sup> chalcogenides,<sup>3</sup> halogenides,<sup>4</sup> etc., and recently to nonlayered compounds such as  $\text{AlN}$ <sup>5</sup> and  $\text{GaN}$ .<sup>6</sup> These nanotubes exhibit great prospects in the fundamental physical sciences as well as modern nanotechnology due to the unique nanotubular structures and quantum confinement effects.<sup>7,8</sup> Stimulated by the novel properties of the nanotubes, other one-dimensional geometries have also become the focus of scientific research, with major progress in nanowires and nanobelts. Thanks to the advancement in the synthetic methods, various nanowires have been obtained

ranging from elementary substances<sup>9</sup> to complex compounds<sup>10</sup> and even to superlattices,<sup>11</sup> while nanobelts are mainly composed of oxides,<sup>12</sup> carbides,<sup>13</sup> and nitrides.<sup>14</sup> Accordingly, some prototypes of advanced nanodevices such as field effect transistors, polarization-sensitive nanoscale photodetectors, and ultra-violet nanowire nanolasers have been developed.<sup>15</sup> In recent few years, nanocones have emerged as a new kind of one-dimensional nanostructure which is superior to nanotubes, nanowires, and nanobelts in some aspects.<sup>16</sup> For example, it is

<sup>†</sup> Department of Chemistry, Nanjing University.

<sup>‡</sup> Department of Physics, Nanjing University.

<sup>§</sup> Zhongshan University.

(1) Iijima, S. *Nature* **1991**, *354*, 56–58.

(2) (a) Chopra, N. G.; Luyken, R. J.; Cherrey, K.; Crespi, V. H.; Cohen, M. L.; Louie, S. G.; Zettl, A. *Science* **1995**, *269*, 966–967. (b) Suenaga, K.; Colliex, C.; Demoncey, N.; Loiseau, A.; Pascard, H.; Willaime, F. *Science* **1997**, *278*, 653–655.

(3) (a) Remskar, M.; Mrzel, A.; Skraba, Z.; Jesih, A.; Ceh, M.; Demšar, J.; Stadelmann, P.; Lévy, F.; Mihailovic, D. *Science* **2001**, *292*, 479–481. (b) Krumeich, F.; Muhr, H. J.; Niederberger, M.; Bieri, F.; Schnyder, B.; Nesper, R. *J. Am. Chem. Soc.* **1999**, *121*, 8324–8331.

(4) Rosenfeld Hacothen, Y.; Grunbaum, E.; Tenne, R.; Sloan, J.; Hutchison, J. L. *Nature* **1998**, *395*, 336–337.

(5) Wu, Q.; Hu, Z.; Wang, X. Z.; Lu, Y. N.; Chen, X.; Xu, H.; Chen, Y. *J. Am. Chem. Soc.* **2003**, *125*, 10176–10178.

(6) Goldberger, J.; He, R. R.; Zhang, Y. F.; Lee, S.; Yan, H. Q.; Choi, H. J.; Yang, P. D. *Nature* **2003**, *422*, 599–602.

(7) (a) *Carbon Nanotubes*; Dresselhaus, M. S., Dresselhaus, G., Avouris, P., Eds.; Springer: Berlin, 2001; pp 117–400. (b) Baughman, R. H.; Zakhidov, A. A.; de Heer, W. A. *Science* **2002**, *297*, 787–792. (c) Tian, Y. J.; Hu, Z.; Yang, Y.; Wang, X. Z.; Chen, X.; Xu, H.; Wu, Q.; Ji, W. J.; Chen, Y. *J. Am. Chem. Soc.* **2004**, *126*, 1180–1183.

(8) Xia, Y. N.; Yang, P. D.; Sun, Y. G.; Wu, Y. Y.; Mayers, B.; Gates, B.; Yin, Y. D.; Kim, F.; Yan, H. Q. *Adv. Mater.* **2003**, *15*, 353–389.

(9) Morales, A. M.; Lieber, C. M. *Science* **1998**, *279*, 208–211.

(10) (a) Chen, C. C.; Yeh, C. C.; Chen, C. H.; Yu, M. Y.; Liu, H. L.; Wu, J. J.; Chen, K. H.; Chen, L. C.; Peng, J. Y.; Chen, Y. F. *J. Am. Chem. Soc.* **2001**, *123*, 2791–2798. (b) Duan, X. F.; Huang, Y.; Cui, Y.; Wang, J. F.; Lieber, C. M. *Nature* **2001**, *409*, 66–69. (c) Guo, L.; Ji, Y. L.; Xu, H. B.; Simon, P.; Wu, Z. Y. *J. Am. Chem. Soc.* **2002**, *124*, 14864–14865. (d) Wu, Q.; Hu, Z.; Wang, X. Z.; Lu, Y. N.; Huo, K. F.; Deng, S. Z.; Xu, N. S.; Shen, B.; Zhang, R.; Chen, Y. *J. Mater. Chem.* **2003**, *13*, 2024–2027. (e) Haber, J. A.; Gibbons, P. C.; Buhro, W. E. *J. Am. Chem. Soc.* **1997**, *119*, 5455–5456. (f) Haber, J. A.; Gibbons, P. C.; Buhro, W. E. *Chem. Mater.* **1998**, *10*, 4062–4071. (g) Zhang, Y. J.; Liu, J.; He, R. R.; Zhang, Q.; Zhang, X. Z.; Zhu, J. *Chem. Mater.* **2001**, *13*, 3899–3905. (h) Liu, J.; Zhang, X.; Zhang, Y. J.; He, R. R.; Zhu, J. *J. Mater. Res.* **2001**, *16*, 3133–3138. (i) Tang, C. C.; Fan, S. S.; de la Chapelle, M. L.; Li, P. *Chem. Phys. Lett.* **2001**, *333*, 12–15. (j) Jensen, L. E.; Björk, M. T.; Jeppesen, S.; Persson, A. I.; Ohlsson, B. J.; Samuelson, L. *Nano Lett.* **2004**, *4*, 1961–1964.

(11) (a) Hu, J. T.; Ouyang, M.; Yang, P. D.; Lieber, C. M. *Nature* **1999**, *399*, 48–51. (b) Gudiksen, M. S.; Lauhon, L. J.; Wang, J. F.; Smith, D. C.; Lieber, C. M. *Nature* **2002**, *415*, 617–620.

(12) Pan, Z. W.; Dai, Z. R.; Wang, Z. L. *Science* **2001**, *291*, 1947–1949.

(13) Zhang, H. F.; Dohnalkova, A. C.; Wang, C. M.; Young, J. S.; Buck, E. C.; Wang, L. S. *Nano Lett.* **2002**, *2*, 105–108.

(14) (a) Wu, Q.; Hu, Z.; Wang, X. Z.; Chen, Y.; Lu, Y. N. *J. Phys. Chem. B* **2003**, *107*, 9726–9729. (b) Bae, S. Y.; Seo, H. W.; Park, J.; Yang, H.; Park, J. C.; Lee, S. Y. *Appl. Phys. Lett.* **2002**, *81*, 126–128.

(15) (a) Huang, Y.; Duan, X. F.; Cui, Y.; Lieber, C. M. *Nano Lett.* **2002**, *2*, 101–104. (b) Wang, J. F.; Gudiksen, M. S.; Duan, X. F.; Cui, Y.; Lieber, C. M. *Science* **2001**, *293*, 1455–1457. (c) Huang, M. H.; Mao, S.; Feick, H.; Yan, H. Q.; Wu, Y. Y.; Kind, H.; Weber, E.; Russo, R.; Yang, P. D. *Science* **2001**, *292*, 1897–1899.

(16) (a) Zhang, G. Y.; Jiang, X.; Wang, E. G. *Science* **2003**, *300*, 472–474. (b) Muradov, N.; Schwitter, A. *Nano Lett.* **2002**, *2*, 673–676.

found that nanocones are more potential candidates for scanning probes and field emitters due to their radial rigidity, which eliminates the poor signals and noise caused by mechanical or thermal vibration.<sup>16a</sup> However, to date the obtained nanocones are still restricted to a very few members such as carbon,<sup>16</sup> boron nitride,<sup>17</sup> silicon carbide,<sup>18</sup> and zinc oxide<sup>19</sup> due to the difficulty in preparation. In this paper, we report on the successful synthesis of quasi-aligned wurtzite AlN nanocones by a chemical vapor deposition technique, and the growth mechanism is briefly discussed.

As an important member of the promising semiconductors of group III nitrides, AlN is characterized by its direct band gap of 6.2 eV, small or even negative electron affinity as well as its high thermal conductivity, excellent chemical stability, and superior mechanical strength. Its nanostructures have been promised a good future in, e.g., flexible pulse-wave sensors, nanomechanical resonators, and light-emitting diodes.<sup>20</sup> In addition, conical structures have been long known for their suitability in field emission due to the strong local electric field at the tips and the unique direction of electron emission. Actually, the invention of Spindt types of Mo and Si cones is the trademark in the history of vacuum microelectronics.<sup>21</sup> Hence, the AlN nanocones reported here not only provide a new member of conical nanostructures, but also serve as a promising candidate for the field electron emitter due to the combination of the small electron affinity and the sharp-tip geometry. The subsequent characterizations of photoluminescence and field emission reveal that these AlN nanocones own a broad blue emission band and a rather good field emission property as expected, suggesting potential applications in light and field emission nanodevices.

## Experimental Section

In a typical run, AlCl<sub>3</sub> and NH<sub>3</sub>/N<sub>2</sub> (NH<sub>3</sub>, 4 vol %) were used as aluminum and nitrogen sources, respectively. An n-type Si(111) wafer was deposited with a 10 nm Ni film via a magnetic sputtering process, and then it was placed in the center of an alumina tube located in a horizontal tubular furnace. The system was evacuated and flushed with Ar several times to remove oxygen and moisture. After the temperature of the furnace was raised to 700 °C, AlCl<sub>3</sub> was vaporized in the front of the tube at 140 °C and subsequently transported by Ar flow (200 sccm) to the reaction zone, where it reacted with NH<sub>3</sub>/N<sub>2</sub> flow (150 sccm) to deposit AlN nanocones on the Ni-coated Si wafer. The reaction lasted for 4 h, and then the system was cooled to ambient temperature under Ar flow. Gaseous AlCl<sub>3</sub> in the exhaust gas was adsorbed by passing through a flask containing alkaline solution to prevent its leakage to the ambient.

The product was characterized by various methods including X-ray diffraction (XRD; Philips X'pert Pro diffractometer), scanning electron microscopy (SEM; JEOL JSM-6300), transmission electron microscopy (TEM; JEOL-JEM-1005), and high-resolution transmission electron microscopy (HRTEM; JEM-40001X). The optical properties of the product were investigated by micro-Raman spectroscopy (T64000 laser

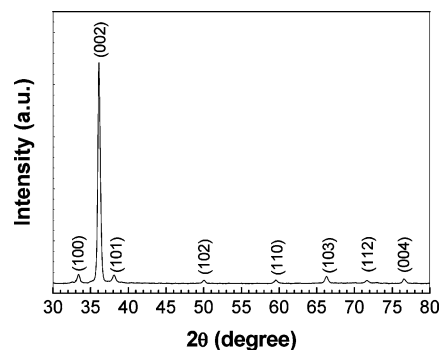


**Figure 1.** XRD curve of the AlN product obtained on a Ni-coated silicon wafer under 700 °C.

Raman spectrometer, excited with an Ar<sup>+</sup> line at 488 nm) and photoluminescence spectroscopy (PL; Amino.Bowman Series-2 spectrometer, excited with a Xe<sup>+</sup> line at 294 nm). The field electron emission measurements were performed by using a parallel-plate configuration in a vacuum chamber at a pressure of  $1 \times 10^{-7}$  Torr.

## Results and Discussion

A typical XRD curve of the product obtained on a Ni-coated Si wafer under 700 °C is shown in Figure 1. All the diffraction peaks can be indexed as the wurtzite AlN phase with lattice parameters  $a = 3.14$  Å and  $c = 4.97$  Å. The strong intensity of the (002) peak indicates that the AlN crystals grew preferentially along the  $c$ -axis; meanwhile the absence of other peaks demonstrates the high purity of our products.

The general morphology of the AlN product was characterized using SEM. From the tilted and cross-sectional views in Figure 2, it is observed that a high density of AlN nanocones grew perpendicularly or slantingly from the wafer to form the quasi-arrays. These AlN nanocones are several micrometers long with linearly decreasing diameters along the growth direction. Further morphological characterization using TEM shows that a typical AlN nanocone has a sharp tip of 20 nm with a smooth surface (Figure 3a). The ripple-like contrast implies the existence of strains along the nanocone. The corresponding HRTEM image (Figure 3b) indicates that the nanocone is a single crystal with a space of 0.266 nm between the neighboring lattice planes, in agreement with  $d_{100}$  space of hexagonal AlN (h-AlN). This confirms that the AlN nanocones grew along the  $c$ -axis as derived from the XRD curve, which is also corroborated by selected area electron diffraction (SAED; Figure 3b, inset). A thin amorphous layer surrounding the outer surface of the AlN nanocone was also observed (Figure 3) as the case for faceted AlN nanotubes, which comes from the surface oxidation in air or the hydrolysis during preparation of the TEM grid.<sup>5</sup>

On the basis of the above analyses, it is seen that the novel quasi-aligned AlN nanocones have been successfully obtained by a moderate chemical reaction. The reaction between AlCl<sub>3</sub> (its vapor pressure is about 50 Torr at 140 °C) and NH<sub>3</sub> catalyzed by a Ni film first resulted in the formation of an AlN film on the wafer.<sup>22</sup> When the film reached a certain critical thickness, AlN nanocrystals were formed because of the inherent strain induced by the lattice mismatch between the AlN and Ni films.<sup>23</sup> The formation of the AlN nanocones could be understood by a vapor–solid epitaxial growth mechanism due to the

- (17) Terauchi, M.; Tanaka, M.; Suzuki, K.; Ogino, A.; Kimura, K. *Chem. Phys. Lett.* **2000**, *324*, 359–364.  
 (18) Wu, Z. S.; Deng, S. Z.; Xu, N. S.; Chen, J.; Zhou, J.; Chen, J. *Appl. Phys. Lett.* **2002**, *80*, 3829–3831.  
 (19) Li, Y. B.; Bando, Y.; Golberg, D. *Appl. Phys. Lett.* **2004**, *84*, 3603–3605.  
 (20) (a) Akiyama, M.; Ueno, N.; Nonaka, K.; Tateyama, H. *Appl. Phys. Lett.* **2003**, *82*, 1977–1979. (b) Cleland, A. N.; Pophristic, M.; Ferguson, I. *Appl. Phys. Lett.* **2001**, *79*, 2070–2072. (c) Kipshidze, G.; Kuryatkov, V.; Zhu, K.; Borisov, B.; Holtz, M.; Nikishin, S.; Temkin, H. *J. Appl. Phys.* **2003**, *93*, 1363–1366.  
 (21) *Vacuum Microelectronics*; Zhu, W., Ed.; John Wiley & Sons: New York, 2001; pp 4–5.

- (22) (a) Wu, N. C.; Tsai, M. S.; Wang, M. C.; Liu, H. S. *J. Cryst. Growth* **2000**, *208*, 189–196. (b) Dollet, A.; Casaux, Y.; Chaix, G.; Dupuy, C. *Thin Solid Films* **2002**, *406*, 1–16.

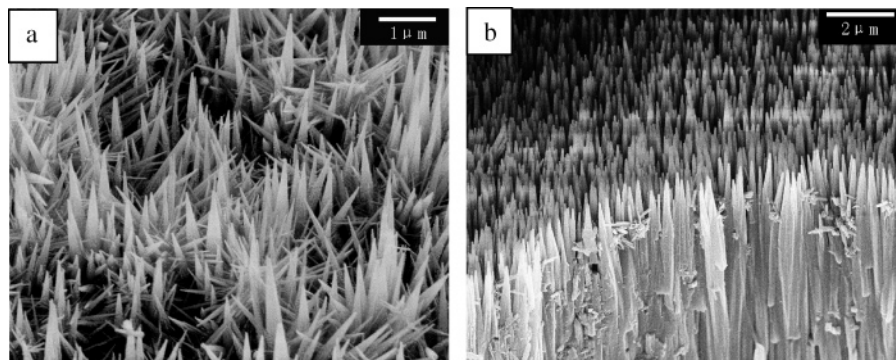


**Figure 2.** SEM images of quasi-aligned AlN nanocones obtained on a Ni-coated silicon wafer under 700 °C: (a) tilted view, (b) cross-sectional view.

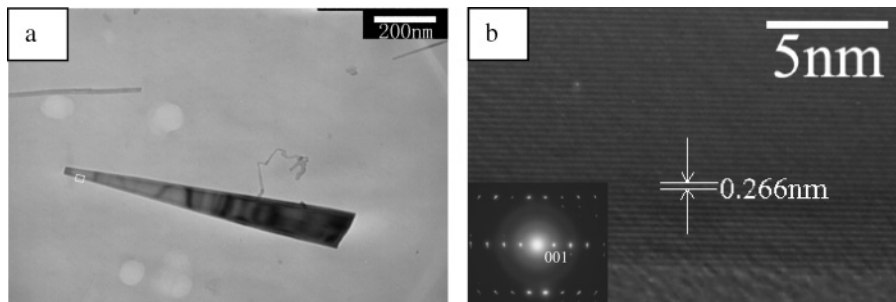


**Figure 3.** TEM and HRTEM images of a typical AlN nanocone: (a) TEM image of an AlN nanocone with a sharp tip of 20 nm, (b) HRTEM image corresponding to the rectangular region in (a). The space of 0.266 nm between the arrows corresponds to the  $d_{100}$  space. The growth direction is along the  $c$ -axis perpendicularly to the (100) plane. The inset is the SAED pattern of the nanocone.

effective steady-state  $\text{AlCl}_3$  vapor pressure.<sup>10e</sup> The inherent asymmetry of the hexagonal crystal structure along the  $c$ -axis of AlN favored the subsequent preferential growth of one-dimensional nanostructures along the [001] direction.<sup>5,24</sup> The morphology of the final product should be dominated by the migration of the newly formed AlN species to the favorable sites on the surface of the preformed AlN nanostructures, where the AlN species might be incorporated into the crystal lattice.<sup>10j</sup> During the growth process, the Ni catalyst stayed on the Si wafer surface and catalyzed the reaction of  $\text{AlCl}_3$  and  $\text{NH}_3$  to continuously produce the AlN species. It seems reasonable to consider that, along the [001] direction of the growing nanostructures, there is a progressive decrease in the amount of the AlN species, leading to the formation of nanocones.

When Ni catalyst was replaced by Fe or Co, quasi-aligned AlN nanocones were still obtained, and even the silicon wafer could be substituted by a quartz wafer, as typically shown in Figure 4a,b. In addition, it is also found that, without catalyst (i.e., using the Si or quartz wafer alone), AlN product in the form of nanoparticles could be formed only at a reaction temperature higher than 850 °C. In contrast, AlN nanocones were easily formed on the catalyst-coated wafers at a reaction temperature as low as 700 °C. Hence, the indispensable function of the catalyst for the formation of AlN nanocones under the present reaction conditions is obvious. Interestingly, raising the reaction temperature leads to the evolution of nanocones to nanocolumns. As can be learned by comparing Figure 3a with Figure 4c, when the reaction temperature was raised from 700

to 750 °C, the tips' dimensions of the AlN nanocones on the Ni-coated Si wafer increased from 20 to 60 nm while the apparent angle between the two edges decreased from 7.5° to 4.0° approximately. AlN nanocolumns were formed (Figure 4d) when the reaction temperature was further raised to 800 °C. These observations are consistent with the above discussions on the formation of the conical shape nanostructures, since a higher temperature could increase the migration rate of the AlN species, promoting a uniform distribution of the AlN species on the surface of the growing nanostructures.

The optical and electronic properties of the AlN nanocones are further examined to explore their promising applications. Since h-AlN belongs to the space group  $P6_3mc$ , six Raman-active modes may be present, i.e.,  $1A_1(\text{TO}) + 1A_1(\text{LO}) + 1E_1(\text{TO}) + 1E_1(\text{LO}) + 2E_2$ .<sup>14a</sup> In the Raman spectrum in Figure 5, two signals at 656 and 614  $\text{cm}^{-1}$  are indexed to the  $E_2(\text{high})$  and  $A_1(\text{TO})$  phonon modes, while a broad small peak at 902  $\text{cm}^{-1}$  is assigned to the overlap of the  $E_1(\text{LO})$  and  $A_1(\text{LO})$  modes.<sup>14a</sup> The peak at 522  $\text{cm}^{-1}$  is originated from the silicon wafer.<sup>25</sup> The weakness and absences of longitudinal optical phonons ( $A_1(\text{LO})$ ,  $E_1(\text{LO})$ ) and another transverse optical phonon ( $E_1(\text{TO})$ ) probably resulted from the special angle between the wave vector of the phonons and the  $c$ -axis of the quasi-aligned AlN nanocones in the near backscattering geometry.<sup>26a</sup> The high-wavenumber shift of  $A_1(\text{TO})$  (614  $\text{cm}^{-1}$ ) compared with that of crystal AlN (610  $\text{cm}^{-1}$ )<sup>14a</sup> might result from the interaction of the polar phonons of the  $A_1$  mode with the long-range electrostatic field, while no wavenumber shift was observed for  $E_2(\text{high})$  due to its nonpolarity.<sup>26b</sup> The

(23) (a) Nesting, D. C.; Kouvetakis, J.; Smith, D. J. *Appl. Phys. Lett.* **1999**, *74*, 958–960. (b) Tamtair, F. G.; Wen, C. Y.; Chen, L. C.; Wu, J. J.; Chen, K. H.; Kuo, P. F.; Chang, S. W.; Chen, Y. F.; Hong, W. K.; Cheng, H. C. *Appl. Phys. Lett.* **2000**, *76*, 2630–2632.

(24) Vayssieres, L.; Keis, K.; Hagfeldt, A.; Lindquist, S. E. *Chem. Mater.* **2001**, *13*, 4395–4398.

(25) Wu, J. J.; Wong, T. C.; Yu, C. C. *Adv. Mater.* **2002**, *14*, 1643–1646.

(26) (a) Lyu, S. C.; Cha, O. H.; Suh, E. K.; Ruh, H.; Lee, H. J.; Lee, C. J. *Chem. Phys. Lett.* **2003**, *367*, 136–140. (b) Bergman, L.; Dutta, M.; Balkas, C.; Davis, R. F.; Christman, J. A.; Alexson, D.; Nemanich, R. J. *J. Appl. Phys.* **1999**, *85*, 3535–3539.

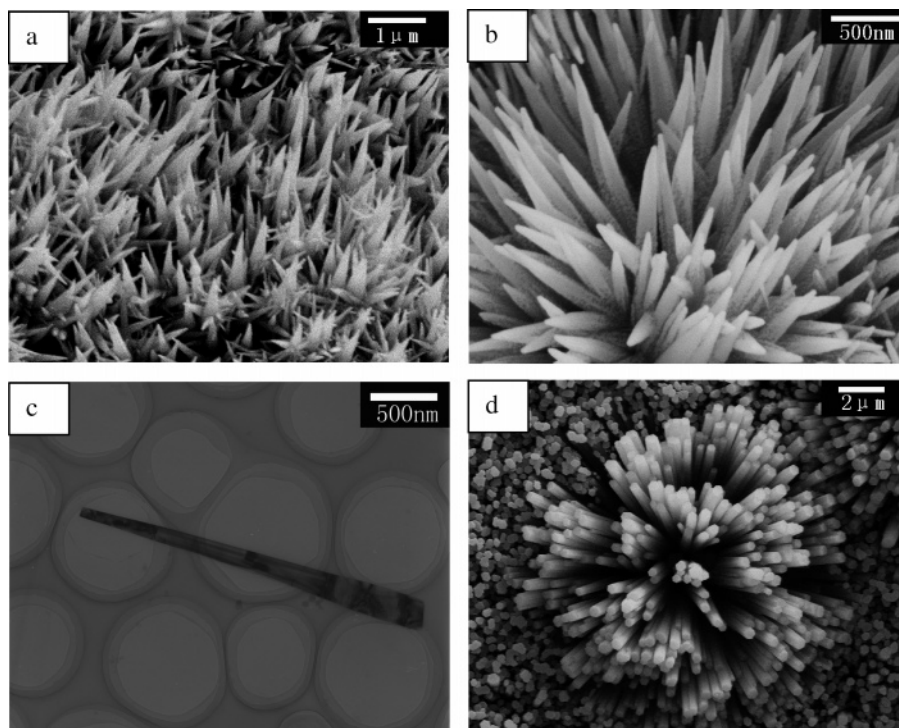


**Figure 4.** SEM and TEM images of quasi-aligned one-dimensional AlN nanostructures synthesized under different reaction conditions: (a) SEM image of AlN nanocones synthesized at 750 °C with a Co-coated Si wafer, (b) SEM image of AlN nanocones synthesized at 750 °C with an Fe-coated quartz wafer, (c) TEM image of a typical AlN nanocone synthesized at 750 °C with a Ni-coated Si wafer, (d) SEM image of quasi-aligned AlN nanocolumns synthesized at 800 °C with a Ni-coated Si wafer.

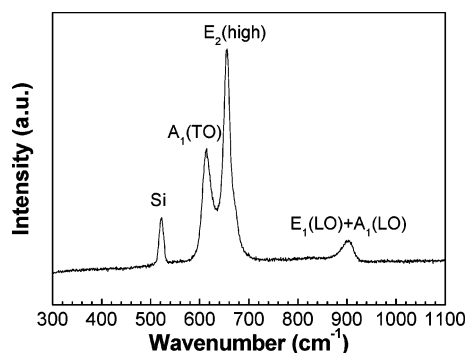


**Figure 5.** Raman spectrum of the quasi-aligned AlN nanocones obtained on a Ni-coated Si wafer under 700 °C.

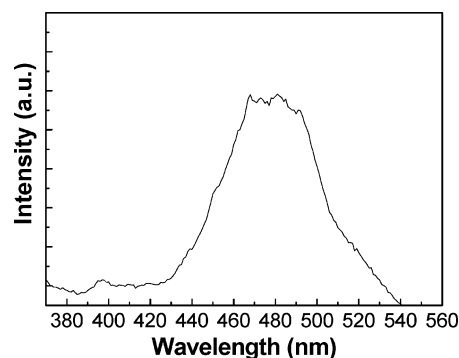


**Figure 6.** Photoluminescence spectrum of the quasi-aligned AlN nanocones obtained on a Ni-coated Si wafer under 700 °C.

broadening and asymmetry of these peaks are due to the nanosized effects and internal strains.<sup>14a,26a</sup>

Figure 6 presents the photoluminescence spectrum of the AlN nanocones, which has a broad blue emission band centered at 481 nm (2.58 eV) with a fine photon structure. Clearly, this band is not the direct band gap emission, but is referred to as a deep-level or trap-level state. In detail, the blue emission originates from the singly ionized nitrogen vacancy in AlN and the radiative recombination of a photogenerated hole with an electron occupying the nitrogen vacancy.<sup>27</sup> In addition, the transitions from shallow donor levels to the excited states of the deep level lead to the fine photon structure.<sup>27b</sup> This indicates that these nanocones have potential applications in blue-light-emitting devices.

(27) (a) Vanheusden, K.; Warren, W. L.; Seager, C. H.; Tallant, D. R.; Voigt, J. A.; Gnade, B. E. *J. Appl. Phys.* **1996**, *79*, 7983–7990. (b) Cao, Y. G.; Chen, X. L.; Lan, Y. C.; Li, J. Y.; Xu, Y. P.; Xu, T.; Liu, Q. L.; Liang, J. K. *J. Cryst. Growth* **2000**, *213*, 198–202.

The field emission measurements of the quasi-aligned AlN nanocones on a Si wafer were performed by using a parallel-plate configuration with a spacing of 0.3 mm in a vacuum chamber at a pressure of  $1 \times 10^{-7}$  Torr. A rather good current–voltage curve with a two-sectional Fowler–Nordheim (F–N) plot was obtained as shown in Figure 7. It is found that the apparent turn-on electric field (defined as the applied field for  $10 \mu\text{A}/\text{cm}^2$ ) was  $12 \text{ V}/\mu\text{m}$ , comparable with that of GaN nanowires deposited on a Si wafer ( $12 \text{ V}/\mu\text{m}$ ),<sup>10a</sup> and the apparent threshold field (defined as the applied field for  $1 \text{ mA}/\text{cm}^2$ ) is estimated to be  $32 \text{ V}/\mu\text{m}$  from the linear fitting in the high electrical field (Figure 7). This is significant for an undoped wide-band-gap material since the field emission properties might be further enhanced with proper doping.<sup>10a</sup> Moreover, a silicon oxide film on the Si wafer surface was unavoidably formed in routine experimental conditions due to the oxygen impurity. Therefore, the intrinsic values of the turn-on and threshold fields of the AlN nanocones should be much lower than the above

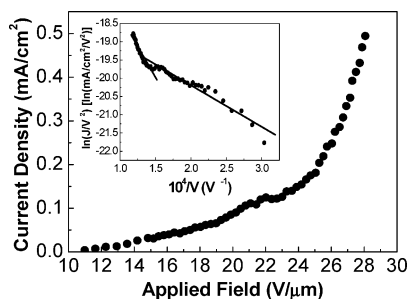


**Figure 7.** Current–voltage curves of the quasi-aligned AlN nanocones obtained on a Ni-coated Si wafer under 700 °C. The inset is the corresponding F–N plots.

apparent values correspondingly, since the silicon oxide film with large resistance on gigaohm order consumed a large portion of the applied voltage. This could be best illustrated by the comparison of the field emission properties of GaN nanorods deposited on a Si wafer and a platinum-coated sapphire wafer.<sup>10a,28</sup> It is seen that the turn-on electric field was greatly reduced from 12 to 0.5 V/μm. These analyses indicate that the obtained quasi-aligned AlN nanocones are indeed a good candidate for the field emitter as expected. The two-sectional feature in the F–N plot (Figure 7, inset) may result from the space charge effect.<sup>29</sup>

(28) Kim, H. M.; Kang, T. W.; Chung, K. S.; Hong, J. P.; Choi, W. B. *Chem. Phys. Lett.* **2003**, *377*, 491–494.

(29) Xu, N. S.; Chen, Y.; Deng, S. Z.; Chen, J.; Ma, X. C.; Wang, E. G. *J. Phys. D: Appl. Phys.* **2001**, *34*, 1597–1601.

## Conclusion

Quasi-aligned wurtzite AlN nanocones on catalyst-coated wafers with the preferential growth direction along the *c*-axis have been successfully synthesized via the reaction between AlCl<sub>3</sub> vapor and NH<sub>3</sub> gas around 700 °C. Effects of reaction conditions such as catalysts, wafers, and reaction temperatures on the morphologies of AlN nanostructures are examined, revealing the possibility of the controllable synthesis of the AlN nanostructures to a certain extent. A vapor–solid epitaxial growth mechanism has been briefly discussed. The unique photoluminescence and field emission properties of these novel AlN nanocones ensure their potential applications in light- and electron-emitting nanodevices.

**Acknowledgment.** This work was financially supported by the National Key Project for High-Tech (Grant No. 2003AA302150), Natural Science Foundation of China (Grant Nos. 20471028 and 50302004), High-Tech Project of Jiangsu Province (Grant No. BG2003029), and Chinese Ministry of Education (Grant No. 02110).

**Supporting Information Available:** A discussion on the growth mechanism of AlN nanocones (PDF). This material is available free of charge via the Internet at <http://pubs.acs.org>.

JA045682V